



Timor Collision Front Segmentation Reveals Potential for Great Earthquakes in the Western Outer Banda Arc, Eastern Indonesia

Aurélie Coudurier-Curveur^{1*†}, Satish C. Singh¹ and Ian Deighton²

¹Institut de Physique du Globe de Paris, CNRS, Université de Paris, Paris, France, ²TGS GPSI, Surbiton, United Kingdom

OPEN ACCESS

Edited by:

Jillian Maloney,
San Diego State University,
United States

Reviewed by:

Gregory Moore,
University of Hawaii at Manoa,
United States
Phil Cummins,
Australian National University,
Australia

*Correspondence:

Aurélie Coudurier-Curveur
acoudurierc@gmail.com

†Present address:

Aurélie Coudurier-Curveur, SNCF
Réseau, DGII, VA OTH, Saint-Denis,
France

Specialty section:

This article was submitted to
Structural Geology and Tectonics,
a section of the journal
Frontiers in Earth Science

Received: 12 December 2020

Accepted: 07 May 2021

Published: 26 May 2021

Citation:

Coudurier-Curveur A, Singh SC and
Deighton I (2021) Timor Collision Front
Segmentation Reveals Potential for
Great Earthquakes in the Western
Outer Banda Arc, Eastern Indonesia.
Front. Earth Sci. 9:640928.
doi: 10.3389/feart.2021.640928

In Eastern Indonesia, the western Outer Banda arc accommodates a part of the oblique Australian margin collision with Eurasia along the Timor Trough. Yet, unlike the Wetar and Alor thrusts of the Inner Banda arc in the north and the adjacent Java subduction zone in the west, both recent and historical seismicity along the Timor Trough are extremely low. This long-term seismic quiescence questions whether the Banda Arc collision front along the Timor Trough is actually fully locked or simply aseismic and raises major concerns on the possible occurrence of large magnitude and tsunamigenic earthquakes in this vulnerable and densely populated region. Here, we jointly analyze multibeam bathymetry and 2D seismic reflection data acquired along the Timor Trough to characterize the location, nature, and geometry of active faults. Discontinuous narrow folds forming a young accretionary prism at the base of the Timor wedge and spatially correlated outcropping normal faults on the bending northwest Australian shelf reveal two concurrent contrasting styles of deformation: underthrusting and frontal accretion. We find that those tectonic regimes and their associated seismic behaviors depend on 1) the thickness of the incoming and underthrusting Cenozoic sedimentary sequence, 2) the vergence of inherited normal faults developed within the continental shelf, and 3) the depth of the décollement beneath the Timor wedge. Based on the along-strike, interchanging distinct deformation style, we identify the mechanical and seismic segmentation along the Banda arc collision front and discuss the implications for earthquake and tsunami hazards along the western Outer Banda arc region.

Keywords: geohazard assessment, Banda arc-continent collision, timor trough, fault segmentation, morphotectonic analysis, 2D seismic reflection data

INTRODUCTION

The deadliest Mw 7.8, 1992 Flores and the Mw 7.5, 2004 Alor earthquakes and tsunamis have forced the scientific community to reassess the geohazards potential in the vulnerable, densely populated coastal Banda arc region (e.g., Harris and Major, 2016; Koulali et al., 2016; Cummins, 2017). These earthquakes occurred on northward verging backthrust north of the Inner Banda arc. However, no such recent earthquakes have occurred along the Outer Banda arc along the Timor Trough. The 21st Century devastating Sumatra and Japan earthquakes have taught us that the absence of recent large earthquakes should not be taken as a guide for future earthquakes, and detailed analyses should be performed.

Performing such an analysis typically relies on the identification of active faults using modern (i.e., instrumental) and past (i.e., historical) earthquake distribution as well as tsunami records

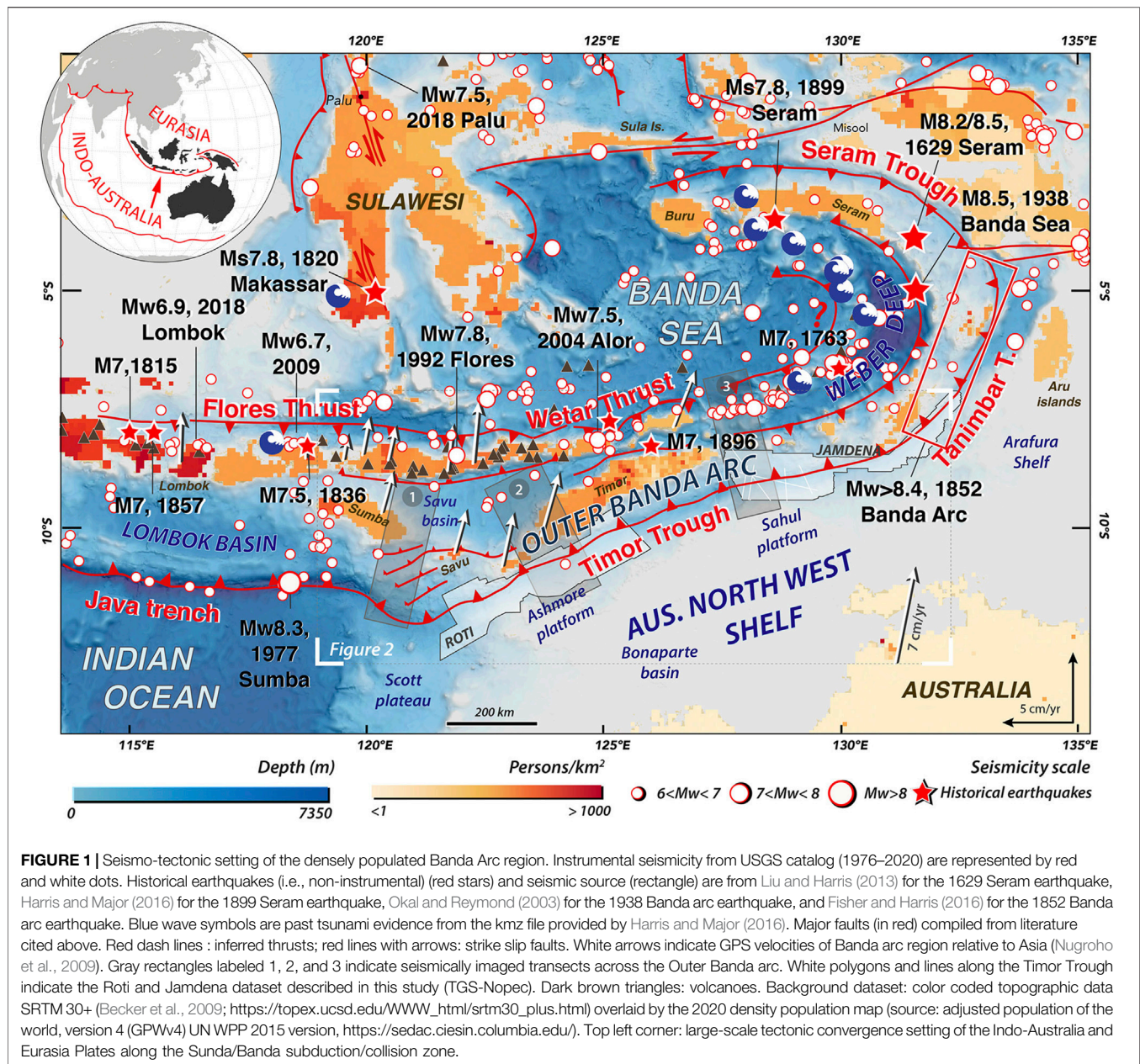


(Figure 1). Present-day seismicity in Eastern Indonesia and Timor Leste is mainly located along the inner, south-dipping Flores and Wetar thrusts—which seemingly localize most of the present-day strain and deformation from the southern collision with the Australian margin (e.g., Genrich et al., 1996; Bock et al., 2003; Nugroho et al., 2009; Koulali et al., 2016)—as well as along the arcuate Seram and Tanimbar troughs further north and eastwards (Figure 1). Historical earthquake records of the past four centuries point toward sources along those same structures, revealing devastating, megathrust earthquakes and tsunamis along the Seram and Tanimbar troughs (e.g., M_{8.2/8.5}, 1629 Seram Trough; M_w > 8.4, 1852 Banda arc; M_{8.5}, 1938 Banda Sea, Figure 1) (Wichmann, 1918; Okal and Reymond, 2003; Liu and Harris, 2013; Fisher and Harris, 2016; Harris and Major, 2016).

In this context, the scarcity of large historical earthquakes alongside a low—almost inexistent—present-day seismicity level along the Timor Trough might be interpreted as an evidence of an inactive and aseismic collision front (e.g., Watt, 1976; McCaffrey and Nabelek, 1984; Genrich et al., 1996). Yet, the Timor collision front likely accounts for more than 2 cm/yr of the oblique Australian convergence indicating that a significant amount of elastic strain energy has been accumulated there for the past 400 years (e.g., Bock et al., 2003; Nugroho et al., 2009; Koulali et al., 2016; Harris and Major, 2016, Figure 1). In this context, the Timor collision front, if active but locked, could represent a major threat for earthquake and tsunami generation for the region (e.g., Nugroho et al., 2009; Liu and Harris, 2013).

To constrain the nature and distribution of the deformation along this modern arc-continent collision example, the Outer Banda arc, some studies have been performed along three main transects located between Sumba and Savu islands (120–121°30'E) (e.g., Breen et al., 1986; Masson et al., 1991; Shulgin et al., 2009), and offshore West and East Timor Island (123–124°30'E and 127°30'–128'E, respectively) (e.g., Karig et al., 1987; Charlton et al., 1991; Hugues et al., 1996) (**Figure 1**). Although varying in style and intensity, the consistent predominant modes of deformation along these transects appear to lie in: 1) frontal accretion processes at the foot of the huge Timor accretionary wedge, where recent trough fill, slope sediments, and/or part of the Australian continental-margin strata are folded and thrust above a décollement (e.g., Breen et al., 1986; Karig et al., 1987; Charlton et al., 1991; Masson et al., 1991; Shulgin et al., 2009; Baillie and Milne, 2014), and 2) sets of deeply rooted normal faults dissecting the Ashmore and Sahul platform sedimentary sequences (e.g., Keep et al., 2002; Barber et al., 2003), locally active in the Quaternary (Hengesh and Whitney, 2016). Although these studies provide some local information along these transects, a detailed characterization of active deformation along the entire Timor Trough is lacking, which is essential for earthquakes and tsunami hazard assessment. For example, we do not know 1) if the frontal accretion is continuous along-strike, 2) if deformation is still active everywhere and most importantly, 3) what are the implications of this deformation style in terms of seismic hazard assessment?

Here, we take advantage of high-resolution multibeam swath bathymetry and 2D seismic reflection data, almost continuously, over more than 700 km of the Timor Trough to expand the investigation of deformation styles and associated faulting along that collision front. These data are generously provided by TGS-NOPEC and were acquired as a part of the “Indonesia Frontier Basins” (IndoDeep) survey in 2007. Our aim is to identify which structures of the Timor collision system possibly accommodate the unaccounted motion of the Australian plate convergence and characterize their significance for earthquake and tsunami hazards. We combine both datasets to identify deformation patterns and constrain active faults both on the incoming Australian northwest (NW) shelf and within the Timor accretionary wedge in two main regions (between 122°E and 126°E and between 128°E and 133°E, dubbed Roti and Jamdena regions, respectively; **Figure 1**). We specifically 1) constrain two distinct tectonic regimes, 2) define a morpho-structural segmentation along the arc-continent collision front, and 3) identify associated active fault sources and their corresponding seismic behaviors. We discuss our results in the global oceanic convergent context to shed light on earthquake and tsunami hazards for the region.

ALONG-STRIKE MORPHOLOGY OF THE TIMOR COLLISION ZONE

Recent Tectonic Setting and Expected Kinematics

The Timor collision front represents the southernmost, youngest deformation front resulting from the ≈8 Myr-old, diachronous

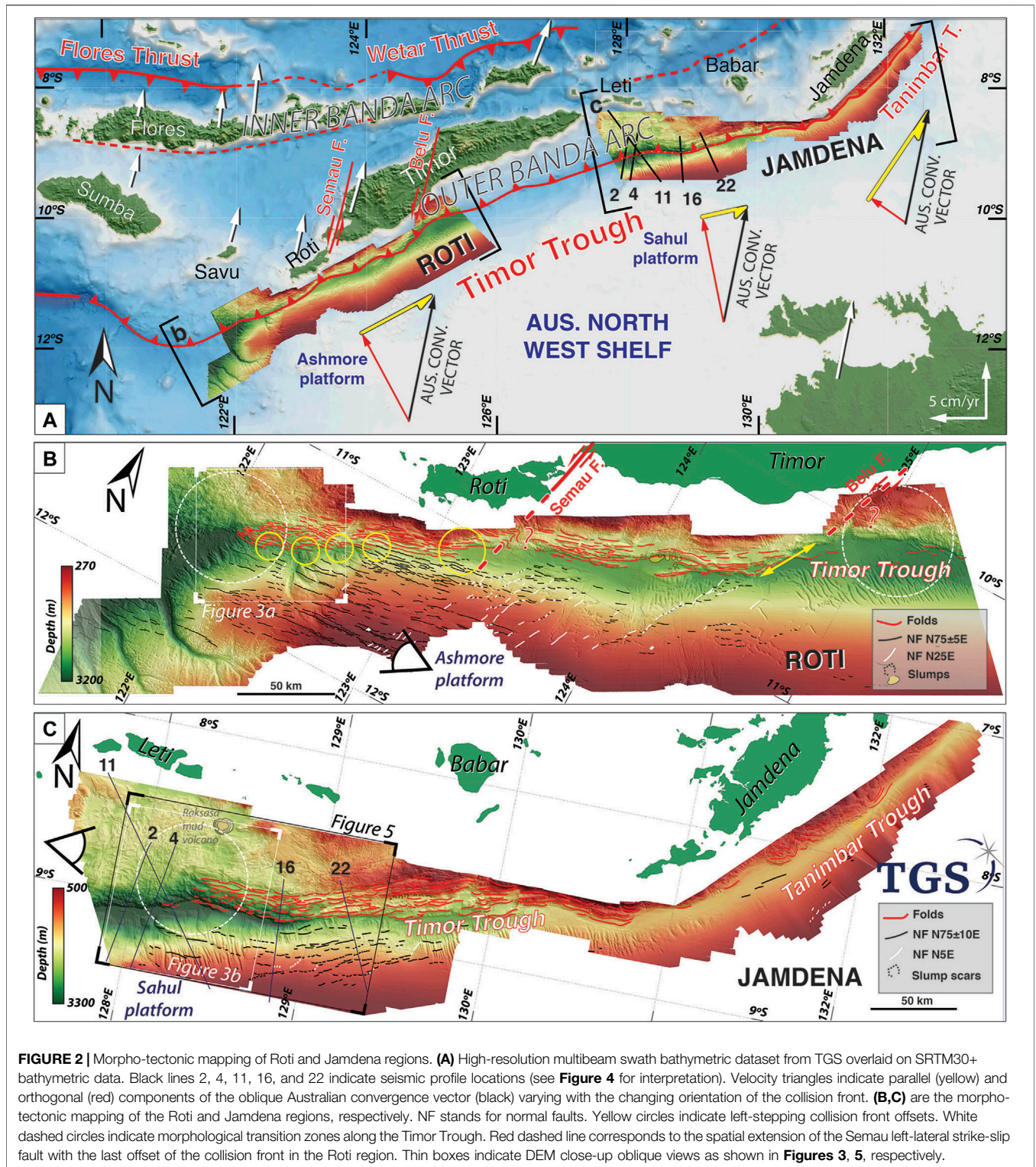
collision between the Australian continental plate and the oceanic domain of the Banda Sea (e.g., Charlton et al., 1991; Hall, 2009; Harris, 2011). This region marks a drastic change in both tectonic processes and nature of converging plates, shifting from an oceanic subduction along the Java Trench to a continental collision along the Timor Trough (e.g., Audley-Charles, 2004). In this region, the Timor collision front bounds a ≈100 km-wide accretionary wedge mainly composed of the northwest Australian shelf sediments. When locally exhumed and uplifted, these sediments outcrop on the Timor, Sumba, Roti and Savu islands (e.g., Roosmawati and Harris, 2009) to form the Outer Banda arc in opposition to the Inner Banda arc, which corresponds to the volcanic arc associated with the initial subduction stage (**Figure 2A**). The Inner Banda arc is the eastward extension of the Java-Sumatra volcanic arc (Norvick, 1979), both resulting from the large-scale convergence of the Indo-Australian plate toward Eurasia. Transitional isotopic and chemical signatures of active and extinct volcanoes along and across the arc reflect spatial and temporal variations in the nature of subducted material and yield evidence for limited to significant continental sediments influence (e.g., van Bergen et al., 1989; Varekamp et al., 1989). Radiometric dating results indicate that continental contamination likely started at least 5 Ma ago in the Wetar/Central Timor region (Elburg et al., 2005; Scotney et al., 2005), which has been interpreted, along with other lines of evidence, as a constraint for the onset of the arc-collision (Harris, 2011).

The obliquity of the Australian convergence in relation to the changing orientation of the Timor collision front entails variable degrees of shortening and strike-slip partitioning, as shown on **Figure 2A**. The margin-orthogonal shortening component is expected to increase from the SW/NE-striking Timor trough section (offshore Savu island to eastern tip of Timor Island, see **Figure 2B**) to the WSW/ESE-striking section (between East Timor and Jamdena Islands, see **Figure 2C**) as the orientation of the collision front becomes nearly east-west. Inversely, the margin-parallel strike-slip component is expected to be larger along the SW/NE-striking Timor trough section than that along the WSW/ESE-striking section, and should definitely become predominant over thrusting along the sub-N/S-striking section of the Tanimbar Trough, running parallel to the N12E Australian convergence vector. Below we discuss the morphology of the Roti and Jamdena regions.

Roti Region

Along the SW/NE-striking Roti region (**Figure 2B**), we identify 1) one main region with elongated, narrow folds oriented N80E on average on the northern side of the Timor Trough, 2) a discontinuous collision front, and 3) two sets of normal faults with azimuths of $N75 \pm 5E$ and $N25E$ dissecting the western Ashmore platform surface south of the trough.

Between 122°E and 124°45'E, narrow folds are almost continuous over the 300 km-long stretch, outlining a more or less well-developed distinctive outer accretionary prism reaching up to 18 km-wide and 800 m-high (profiles R2 and R3 in **Figure 3A**). They likely accommodate several tens of kilometers of shortening of incoming NW shelf material at the



foot of the Timor wedge. Where the folded section is shorter, the folds form a low (200 m-high) topography at the foot of the kilometeric-scale structural step as if recently added to a pre-existing wedge (R2 profile offshore in **Figure 3A**). West and east of this folded stretch (between

121°45'E and 122° and between 124°45'E and 125°10'E), the wedge morphology changes rather abruptly, exhibiting a rugose texture similar to the morphology of the upper wedge seen above the prominent folds (**Figures 2B, 3A**). However, both folded and rough regions show a consistent, first-order

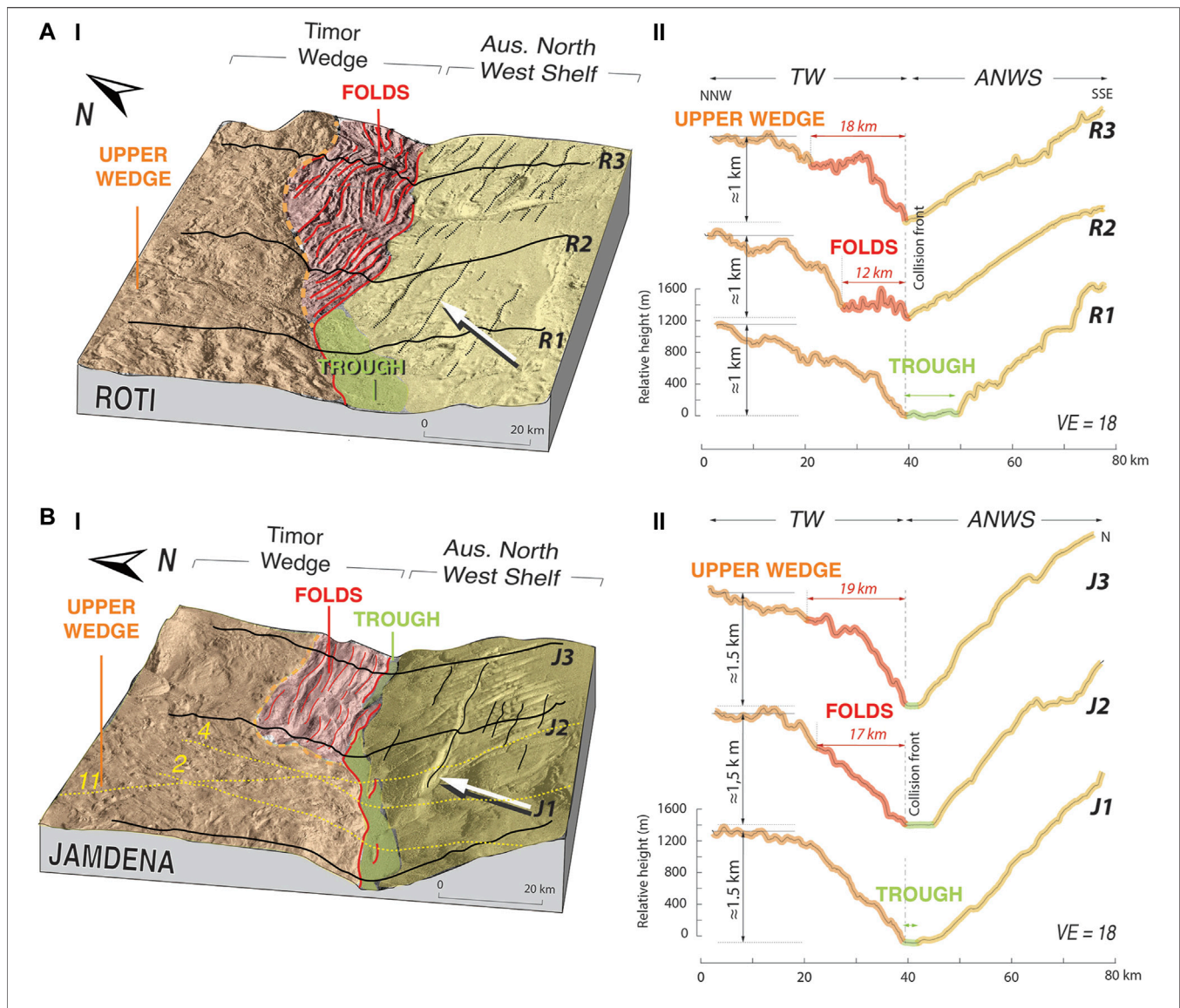


FIGURE 3 | Morphology and topography of morpho-tectonic transition zones offshore West Timor and Roti island **(A)** and offshore East Timor and Leti islands **(B)**. **(I)** Oblique views of the high-resolution bathymetric datasets with morpho-tectonic interpretation (See location in **Figure 2**). White arrows indicate Australian convergence direction. **(II)** Bathymetric profiles R1-R3 and J1-J3 are from Roti and Jamdena areas, respectively, with corresponding morpho-tectonic interpretation. TW, Timor Wedge; ANWS, Australian North West Shelf. In both **(A,B)**: Incoming, faulted Australian sediments, flat trough sediments, prominent folds of the lower wedge, and undeformed upper wedge are highlighted in yellow, green, red, and orange, respectively. Orange dash line indicates the boundary between the upper wedge “rough region” and the “folded region”. Note the clear left-stepping deformation front offshore west Timor and Roti islands **(A)** as identified in **Figure 2**. Note also the spatial correlation between NW shelf normal faults location/orientation and regions where prominent folds have developed at the foot of the Timor Wedge in both areas. Width of the folded section shows a gradual increase in Roti region and reaches a maximum of about 20 km in both regions.

kilometric-scale topographic step as well as a convex-upward front (**Figure 3A**).

Along the first western 100 km of the folded stretch, the N60E-oriented deformation front shows several, kilometric left-stepping offsets ranging between 5 and 15 km (**Figures 2B, 3A**), which likely accommodate the kinematically expected strike-slip component of the Australian convergence as described above. We do notice Z-shaped features east of that offset, around 123°10'E, aligned with a geographic step between the Roti and Timor coastlines (**Figure 2A**) and coinciding with

the location of the Semaui left-lateral strike-slip fault, which has been proposed to transfer most of the plate convergence from the collision front to the inner arc structures (e.g., Nugroho et al., 2009; Koulali et al., 2016).

The N75 ± 5E-oriented normal fault set is well-developed in the western part of the Roti dataset and dissects the regularly steepening Australian northwest shelf surface over more than 300 km along and 100 km away from the collision front. These normal faults are spatially correlated with the folds location (i.e., in the convergence direction) (**Figures 2B, 3A**). The

N25E-oriented normal faults, sub-parallel to the convergence direction, are visible over a 150 km long section, east of the Semau Fault location and west of the possible offshore continuation of the Belu strike-slip fault. These faults are predominant over the N80E normal faults forming N25E “en échelon” fault arrays exhibiting strike-slip accommodation processes. Between 124°E and 124°30'E, a nearly continuous, 80 km-long en-échelon array correlates with a major shift, or left-stepping offset, of the collision front location northeastwards and with the possible offshore continuation of the Belu strike-slip fault, which might also contribute to plate convergence transfer to the Inner Banda arc structures. This significant en-échelon array marks an abrupt morphological change in the northwest shelf eastwards, followed by a smooth, nearly undisturbed morphology. Note a few narrow folds have developed in the Timor wedge in this region.

Jamdena Region

Further east, along the WSW/ESE-striking Jamdena region, we identify very similar tectonic features to those observed in the Roti region: 1) a frontal wedge region marked by elongated folds, however, here, associated with 2) a rather continuous collision front, and 3) two sets of normal faults dissecting the Sahul platform surface (Figure 2C). Between 128°20'E and 130°30'E, broad-folds oriented N95E–N70E, i.e., roughly parallel to the collision front, form a distinctive accretionary prism north of the Timor Trough (Figure 2C), nevertheless less prominent than that in the Roti region (Figure 2B). The width of the folded region reaches 19 km throughout this area (Figure 3B). As described in the Roti dataset, the folded region forms part of a kilometric-scale structural step exhibiting a steeper frontal slope compared to those offshore West Timor and Roti Islands ($\approx 4.3^\circ$ and $\approx 2.3^\circ$, respectively), as is observed in the incoming margin slope (Figure 3B). West of this folded region, the Timor wedge morphology changes abruptly to a rather heterogeneous morphology, marked by a rugged texture (particularly visible between 127°40'E and 128°25'E up to the front) as previously described in the Roti region. The nearly continuous deformation front does not feature any clear left-stepping offsets here, as expected in relation to the changing orientation of the collision front (Figure 2A). Two sets of normal faults are visible on the incoming Australian margin with comparable azimuths to those observed in the Roti region (N75 \pm 10E and N5E, respectively). However, their seafloor imprint is more subdued here and the N5E-oriented en-échelon fault array is very restricted. Note here again a spatial correlation between the normal faults developed in the northwest shelf and the outer folds of the Timor wedge.

ANATOMY OF THE TIMOR COLLISION FRONT ZONE

2D Seismic Dataset

To constrain the nature and geometry of underlying fault systems contributing to the variable morphologies described in the Timor wedge and in the Australian northwest shelf, we interpret and correlate five high-resolution 2D seismic reflection profiles acquired offshore East Timor and Leti Islands (i.e., in Jamdena

region, Figures 2, 3) (Figures 2, 3). The five profiles (MH07-02, MH07-04, MH07-11, MH07-16, and MH07-22, dubbed profiles 2, 4, 11, 16, and 22, respectively, in the following) image both the Australian northwest shelf and the Timor wedge between 128°E and 129°20'E, over spatial lengths ranging between 72 and 150 km, and record lengths of 8–12 s two-way travel time (TWT).

We map a series of prominent sedimentary reflectors on the northwest Australian shelf (Figures 4A,B) that we correlate with a few published known horizons identified in this area (e.g., Keep et al., 2002; Baillie et al., 2004, see Supplementary Figure S1) with observed reflectors analyzed here to delimit the Cenozoic sedimentary section (Figures 4A,B). In the Timor wedge, we map three main seismic units: 1) an undeformed, thick bright unit (300 ms TWT on average, see Figures 4A,B) likely indicating pelagic or semi-pelagic sediments (e.g., Breen et al., 1986) on top of 2) a chaotic reflection of likely intensively deformed old sediments representing the upper wedge of the rugged regions, and 3) a series of parallel reflectors characteristic of the Cenozoic sedimentary section either observed continuously beneath the rigid upper wedge (e.g., profile 4, Figures 4A) or intensively stacked atop one another at the front of the Timor wedge (e.g., Figures 4B,Bii). We finally map normal and thrust faults from the edge of the Sahul platform to the upper Timor wedge (Figures 4A,B).

Along-Strike Structural Variations

The northwest Australian shelf exhibits clear, flat and parallel reflectors changing from being sub-horizontal on the Sahul platform to north-dipping in the downgoing northwest shelf slope (Figure 5). The overall thickness of this Cenozoic sedimentary sequence at the collision front increases significantly from the western profiles to the eastern ones (i.e., reaches about 1.5 s TWT on profile 2 vs. 3 s TWT along profile 22, Figures 5, 6). Most of the reflectors are regularly disturbed by sets of conjugate normal faults, extending to the lowermost strong reflection (likely being the top of the Triassic unit, Keep et al., 2002). The deeper and older units show constant thickness and fault offsets attesting pre-tectonic deposition while the upper units (i.e., younger than Pliocene) exhibit syn-tectonic deposition as recorded by larger deposition centers along and between antithetic normal faults indicating a recent increase in fault activity (Figures 4, 5). Some of these normal faults locally outcrop at the seafloor forming the \approx N75E-striking normal faults we have described above, particularly noticeable along profile 22.

Toward the Timor wedge, the downgoing Cenozoic section on profiles 2 and 4 shows mostly landward-verging normal faults over the entire profile lengths. The abrupt change of seismic reflection signal between the parallel reflectors and the chaotic wedge unit (Figure 4A) indicates the location of a single, shallow-dipping frontal decollement extending for at least 20 km north of the deformation front (Figures 4, 5). This thrust bounds both the base of the consolidated, inactive upper wedge, where no clear structure nor recent folding can be seen, and on top of which the thick bright pelagic cover extends over the entire wedge width. The profile 11 shows a similar wedge architecture to profiles 2 and 4 with an additional sedimentary section at the foot of the accretionary wedge, involving the youngest Cenozoic

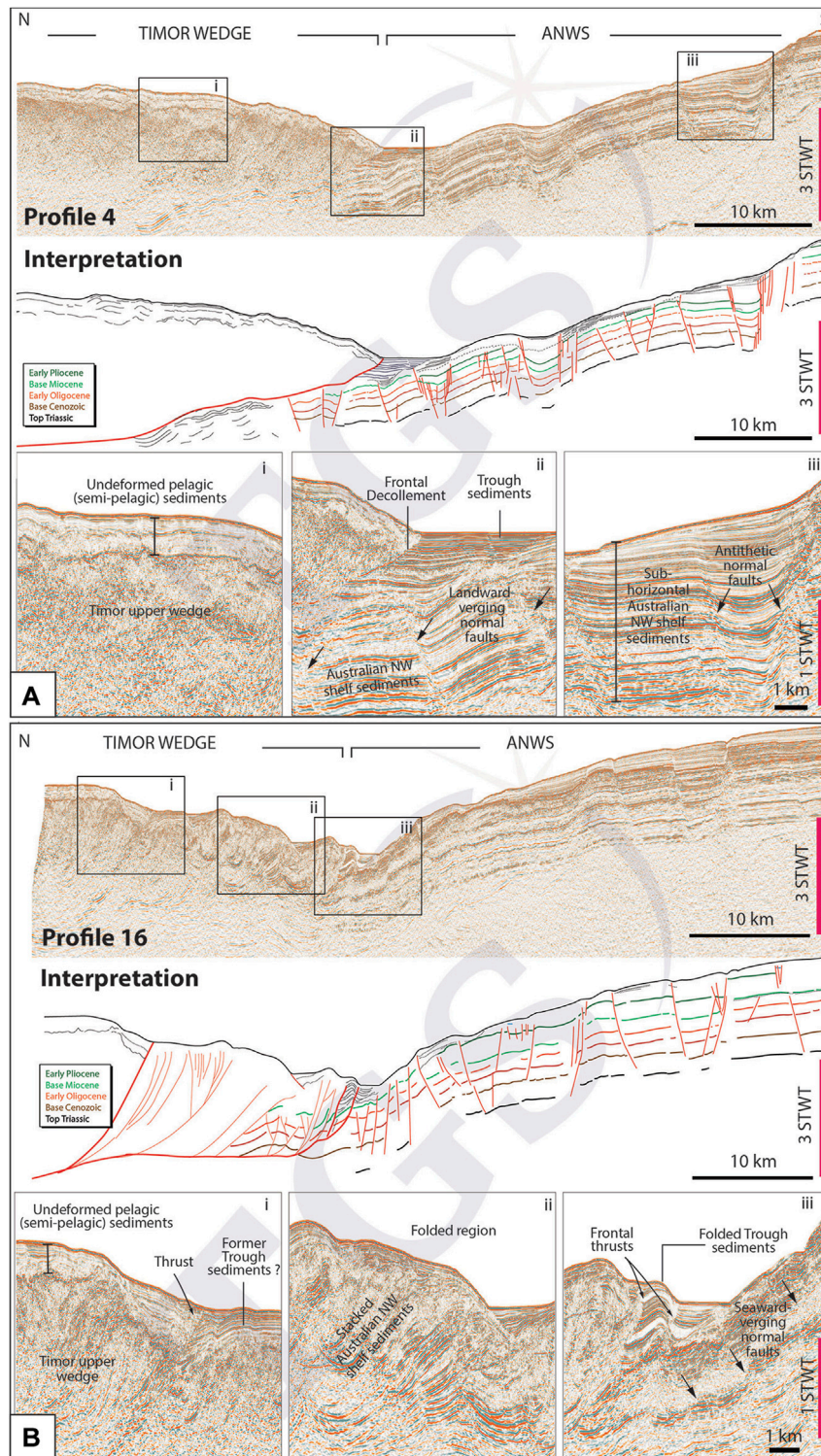


FIGURE 4 | High-resolution seismic reflection data across the Timor Trough of seismic profiles 4 (A) and 16 (B) (see location on Figure 2). Top images in both (A,B) show non-migrated seismic profiles. Middle images show corresponding horizon and fault interpretations. Colored lines represent the different horizons correlated with published seismic line interpretations in the Australian northwest shelf (see Supplementary Figure S1). Faults are indicated in red. Bottom images show three local close-up views (i–iii) highlighting the characteristic seismic units identified along those profiles. Seismic reflection data are generously provided by TGS-Nowep, acquired as part of the “Indonesia Frontier Basins” (IndoDeep) project.



FIGURE 5 | Along-strike variations of the morphology, fault geometry, and thickness of incoming Australian sediments along the collision front in Jamdena region. Interpreted seismic profiles MH07-02, MH07-04, MH07-11, MH07-16, and MH07-22—dubbed 2, 4, 11, 16, and 22—with corresponding bathymetry. Faults within the incoming margin and Timor Wedge in red and black, respectively. Main thrust indicated by the thick red line. Main horizons in thick colored lines. Extended interpretation in dashed black lines within and under the Timor Wedge. Cenozoic sedimentary sequence represented from red to yellow units. Similar horizontal and vertical scales apply to all five profiles.

sedimentary units as well as the Trough sediments (Figure 5). On profiles 16 and 22 (Figure 5), the thick incoming Cenozoic sequence displays both landward and seaward-verging normal

faults. The latter show reverse reactivation close to the front. Differing from profiles 2 and 4 (Figure 5), these sediments are not observed under the Timor wedge but observed as part of it,

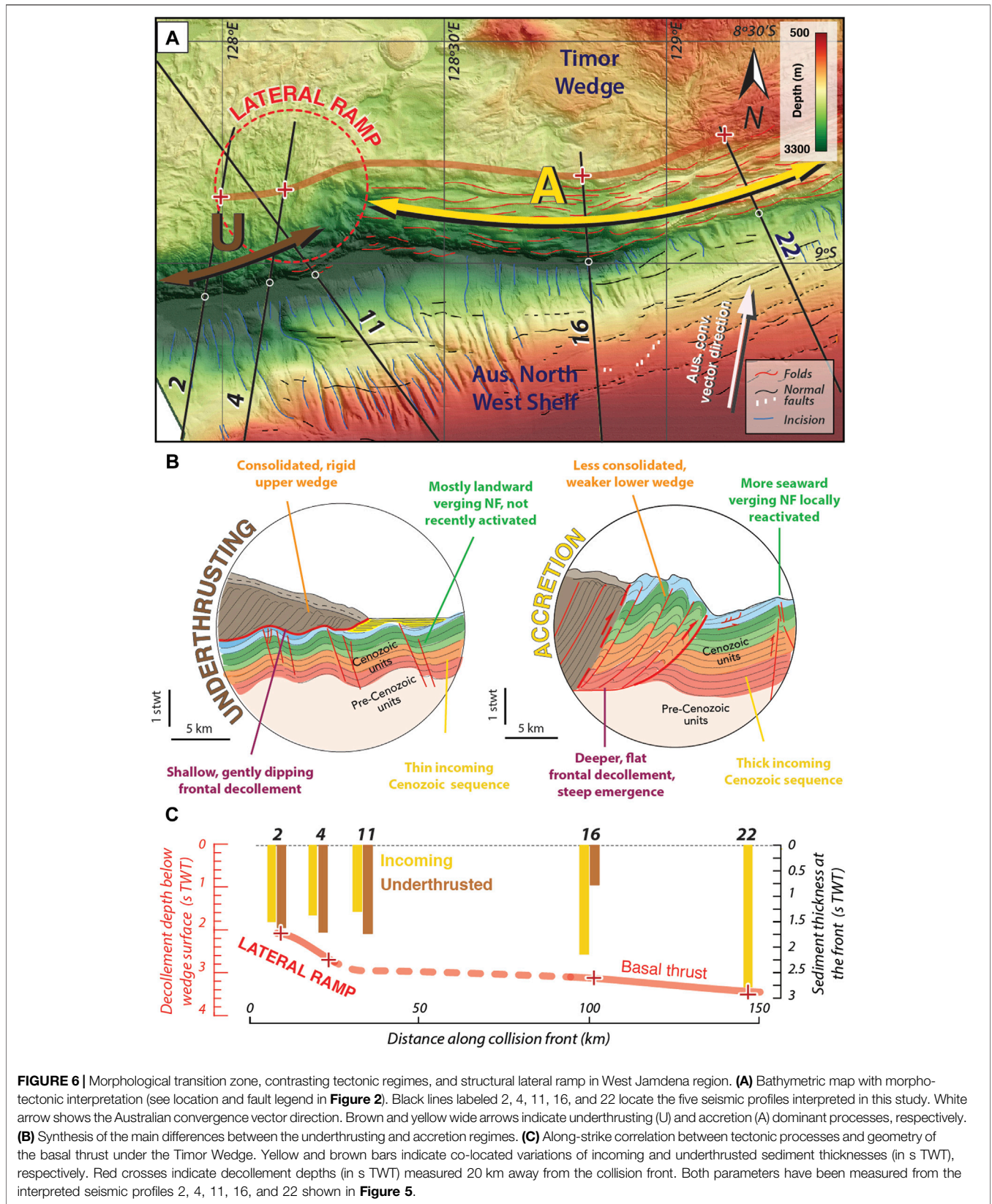


FIGURE 6 | Morphological transition zone, contrasting tectonic regimes, and structural lateral ramp in West Jamdena region. **(A)** Bathymetric map with morpho-tectonic interpretation (see location and fault legend in **Figure 2**). Black lines labeled 2, 4, 11, 16, and 22 locate the five seismic profiles interpreted in this study. White arrow shows the Australian convergence vector direction. Brown and yellow wide arrows indicate underthrusting (U) and accretion (A) dominant processes, respectively. **(B)** Synthesis of the main differences between the underthrusting and accretion regimes. **(C)** Along-strike correlation between tectonic processes and geometry of the basal thrust under the Timor Wedge. Yellow and brown bars indicate co-located variations of incoming and underthrustsed sediment thicknesses (in s TWT), respectively. Red crosses indicate decollement depths (in s TWT) measured 20 km away from the collision front. Both parameters have been measured from the interpreted seismic profiles 2, 4, 11, 16, and 22 shown in **Figure 5**.

displaying thin wedge slices stacked atop one another along long, steep thrusts rooted on a relatively deep horizontal basal decollement. They form rather unconsolidated, weaker, recent folded morphology described earlier, in opposition to the old rigid upper wedge described on profiles 2 and 4 (Figure 5). The outer wedge in this section is not topped by the undeformed pelagic (or semi-pelagic) sediment layer described above. That sedimentary layer actually stops where the first, inner, steep slice of Cenozoic sediments starts being accreted to the old upper wedge (see Figures 4B, 5).

DISCUSSION: CONSTRAINTS FOR FUTURE GEOHAZARD ASSESSMENT

Two Contrasting Tectonic Regimes

Our morphological, topographic, and seismic data analyses reveal two distinct tectonic regimes varying from total underthrusting to total accretion, which are seemingly controlled by inherited structures of the northwest shelf in the Jamdena region (Figures 5, 6A). Based on similar morphological characteristics highlighted both on the northwest Australian shelf and in the Timor wedge, we assume that comparable tectonic wedge architectures and tectonic regimes lie in the Roti region as well, for which we do not have any seismic constraints. The underthrusting regime is characterized by 1) the total underthrusting of a rather thin section of incoming Cenozoic sediments (Figures 6B,C), exhibiting mostly landward-verging normal faults, 2) a single, low-dipping shallow decollement (Figures 6B,C), and 3) a consolidated, rigid, and non-recently deformed upper wedge (see also profiles 2 and 4). The accretion regime is characterized by 1) the total accretion of a rather thick section of the incoming Cenozoic sediments (Figures 6B,C), exhibiting more seaward-verging normal faults, 2) a deep frontal decollement with steep frontal thrusts (Figures 6B,C), and 3) the development of an unconsolidated lower accretionary wedge in front of the older wedge (profiles 16 and 22).

Close to the deformation front, some of the seaward-verging normal faults cutting the entire sediment thickness show thrust reactivation (profile 22, Figure 5), indicating that the growth of the recent accretionary prism likely uses pre-existing, favourably oriented normal faults of the incoming northwest shelf sediments. The spatial distribution and similar orientation of both the N75E faults developed in the northwest shelf and the narrow folds of the accretionary prism along the collision front in the Jamdena region (Figures 2, 3) support this hypothesis. It is also possible that these prevailing tectonic regimes give evidence for different, but concurrent, chronological stages of deformation along the collision front where the Timor wedge evolves from a nascent collision stage to a more mature stage as it incorporates a developing accretionary prism. This would be in keeping with the larger time and space scale diachronous growth and exhumation of the Banda arc islands, influenced by the shape (e.g., Scott plateau protrusion) and sedimentary structure of the incoming Australian shelf (Keep et al., 2002; Harris, 2011).

The morphological and structural transition from the underthrusting to the accretion regime is associated with a

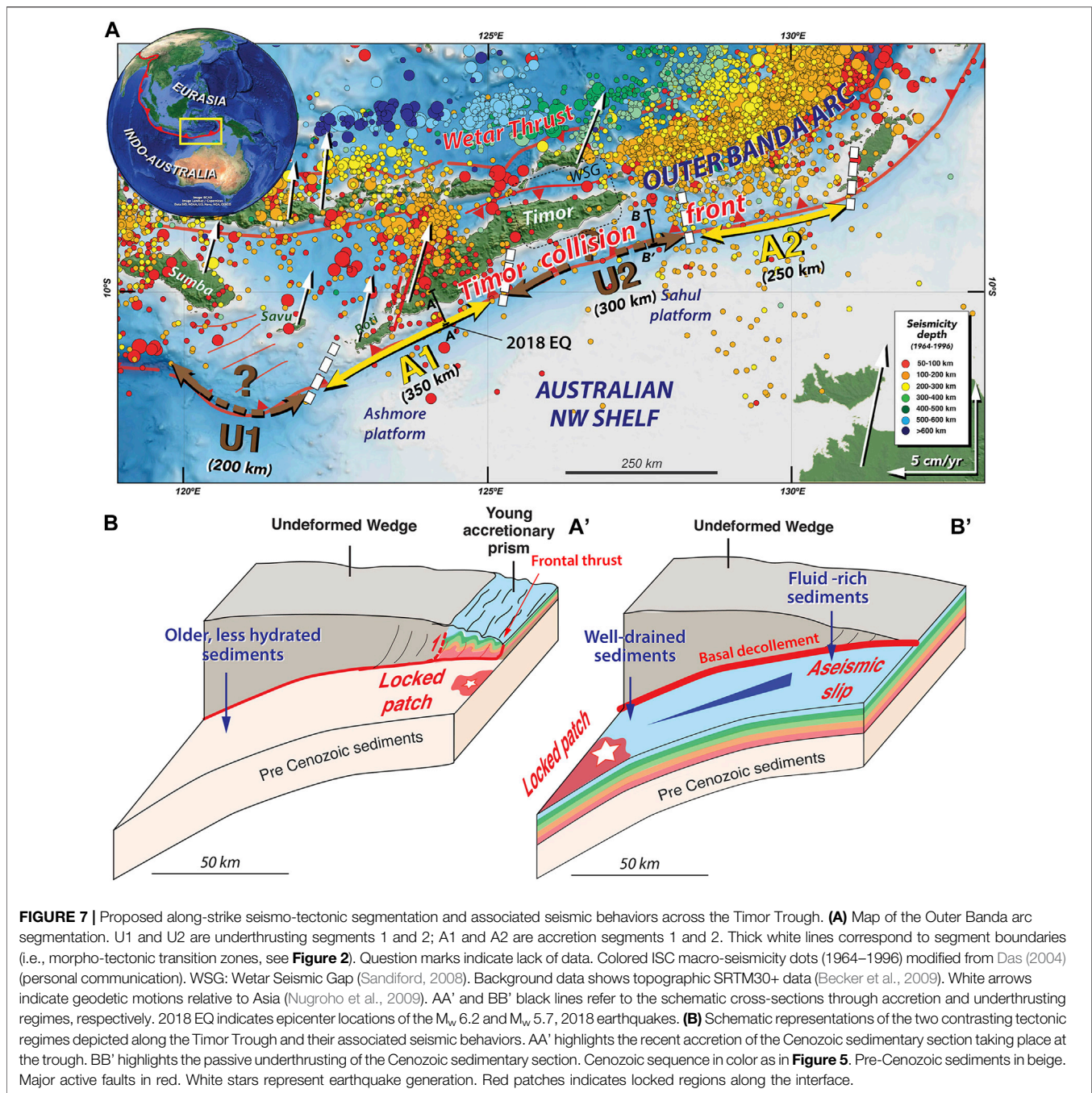
decollement depth increase (from 2 s TWT to almost 4 s TWT, Figure 6C) thus forming a structural step that one could consider a lateral ramp (Tréhu et al., 2019). If significant enough, lateral ramps can act as barriers to slip propagation (e.g., Qiu et al., 2016—Himalayan range). Morpho-structural transitions can therefore be used to infer fault segmentation along the Timor Trough, which indirectly helps constraining geohazards—earthquake magnitude being directly related to the rupture area.

Fault Segmentation, Seismic Behavior, and Active Fault Sources

Along the Timor wedge, we identify four morphological transition zones (located around 122°E, 125°10'E, and 128°20'E, and 131°E along the collision front, Figure 7), likely indicating tectonic regimes shifts and therefore structural variations (i.e., lateral ramps). We characterize four fault segments, which alternate between underthrusting and accretion dominated processes along most of the Timor Trough segment of the Outer Banda arc (Figure 7). The two accretion segments A1 and A2 are 350 km and 250 km-long, respectively. The lengths of U1 and U2 underthrusting segments are 200 and 300 km, respectively, which are maximum values since we do neither have bathymetric nor 2D seismic data in those fault segments to verify the absence of other structural complexities constraining smaller segments. The two shallow aseismic underthrusting segments U1 and U2 spatially correlate with two relatively quiet seismic zones of the intermediate seismicity as shown on Figure 7 (ISC catalog : 1964–1996, relocated hypocenters shown for earthquakes deeper than 50 km, Das, 2004 – personal communication, Figure 7), including the Wetar Seismic Gap identified as a slab window (Sandiford, 2008; Ely and Sandiford, 2010) (Figure 7). This spatial correlation between shallow and deeper processes suggests that the present-day collision front segmentation we propose here reflects the large-scale and long-term geodynamics of the collision between the northwest Australian shelf and the Outer Banda arc.

In relation to the differences in the fault geometry, thicknesses of underthrust sediments, and overall tectonic structure of the Timor wedge, the underthrusting and accretion segments are likely experiencing different seismic behaviors. In the following, we refer to subduction examples rather than collision ones in an attempt to constrain those behaviors. In the absence of local geodetic and geochemical investigations to directly constrain the interface seismic state, we do take advantage of intensive investigations published on analogous oceanic convergent settings (e.g., Moore et al., 2007; Kodaira et al., 2012; Han et al., 2017; Kodaira et al., 2017; Li et al., 2018; Tréhu et al., 2019; Von Huene et al., 2019; Olsen et al., 2020; Watson et al., 2020).

In the accretion segments, the lack of high-fluid content, young Australian Cenozoic sediments under the wedge indicates that the basal thrust would be relatively strong (i.e., with a relatively high-seismic coupling) and therefore not that prone to regular great earthquakes nucleation at depth, but likely regularly rupturing with smaller magnitude earthquakes (Figure 7; Li et al., 2018). This would be consistent with the



moderate ($M < 6.5$) seismicity recorded in both Jamdena and Roti regions. The largest of these moderate magnitude earthquakes—with magnitudes of M_w 6.2 and M_w 5.7—successively occurred offshore west Timor Island on August 28, 2018 (**Figure 7**; **Supplementary Figure S2**) on a 68° north-dipping plane at 14 km depth and on a 33° north-dipping plane at 8 km depth, respectively (**Supplementary Table S1**). Epicentre locations and focal mechanisms from the USGS catalog suggest that the larger one likely reactivated one of the relatively steep, pre-existing, favourably oriented normal fault as a

thrust fault (see **Supplementary Figure S2**), and that the smaller one, ruptured the most frontal thrust of the recent Timor wedge. Slump traces mapped in the vicinity of those faults (**Figure 2B**) might result from shaking during those two earthquakes and could therefore be good indicators of recent earthquakes in the region. In combination with our morpho-tectonic and structural observations, we therefore envision three types of active fault sources for the accretion segments: 1) the most frontal thrust of the Timor wedge, 2) the incoming, thrust-reactivated normal faults, and 3) the backstop thrust (or

megasplay), which represents a mechanical boundary between the old, stronger wedge and the newly, weaker and fluid-rich segment (Moore et al., 2007) (Figure 7, line AA'). Because of their relative steepness (note that we do not derive any dip measurement from the time sections), slip along these faults could result in significant seafloor uplift and subsequent tsunami waves even for moderate earthquakes (Singh et al., 2011).

In the underthrusting segments, the overall high-fluid content of a relatively thick, young Australian Cenozoic sediment sequence passing beneath the rigid upper wedge, would likely generate elevated pore pressure on the basal decollement, resulting in the weakening of thrust (Han et al., 2017) (Figure 6). The absence of deformation in the overlying wedge supports the possibility of a weak basal thrust (e.g., Tréhu et al., 2019). Such a mechanical weakening would favor stable sliding at shallow depths (Li et al., 2018), which, in the Timor region, possibly accounts for the present-day, nearly aseismic behavior of the Banda arc collision front (Figures 1, 7). However, progressive dewatering and consolidation of the Cenozoic sediments at greater depths (i.e., at elevated temperature and pressure) could result in the formation of a large, uniform locked asperity where nucleation of regular and great earthquakes could take place (Ruff, 1989; Li et al., 2015; Li et al., 2018) (Figure 7, line BB'). Such a rupture could either be restricted to the deeper portion of the basal thrust or extend up to the front. In the first case scenario, the stable sliding shallow area, seemingly weakly coupled, might impede updip co-seismic slip propagation as characterized for the M_w 7.8, 2016, Pedernales (Ecuador) and the M_w 7.6, 2012, Costa Rica earthquake rupture patterns (Dixon et al., 2014; Rolandone et al., 2018, respectively). In the latter case, that same conditionally stable shallow basal thrust area could become unstable and prone to rupture under certain circumstances (Scholz and Campos, 2012). This process possibly explains the unexpected trench-rupturing M_w 9.0, 2011, Tohoku Oki earthquake Japan, 2011 (Kodaira et al., 2012) and the M_w 8.4, 2010, Maule earthquake (Tréhu et al., 2019). The main active fault of the 200–300 km length consisting of underthrusting segments with locked basal decollement, which accommodates most of the convergence, and could possibly generate large magnitude earthquakes and tsunamis (Figure 7, line BB').

CONCLUSION

The Timor Trough stands out in the Banda arc region as the most seismically quiet region from both an instrumental and historical point of view, despite nearly accommodating 30% of the convergence between Australia and Eurasia. This apparent contradiction questions whether the Timor collision zone is able to produce great earthquakes in an even longer time frame than existing recordings or whether it is simply inactive. Morphology and structural architecture of the Timor wedge constrain two prevailing tectonic regimes for the Australian convergence accommodation (i.e., total accretion and total underthrusting of incoming Cenozoic sediments) exhibiting alternating segments of about 200–350 km-long, separated by lateral ramps along the Timor Trough. Accretion and stacking of the Cenozoic sedimentary sequence in a distinctive outer accretionary wedge is likely associated with moderate magnitude earthquake generation on steep faults located both

within and near the collision front. Long-term underthrusting of the entire young, Cenozoic sedimentary sequence seems to control the along-dip seismic behavior of these segments, possibly enhancing locked patches generation at depth because of the dewatering processes, which could rupture in great earthquakes up to the trough. Our findings highlight the existence of a significant tectonic threat for the western Banda arc region, which could serve probabilistic geohazard models in order to facilitate better risk management in Indonesia.

DATA AVAILABILITY STATEMENT

The data analyzed in this study is subject to the following licenses/restrictions: The datasets shown in this study are confidential. However, we are able to provide a digital copy of the images shown in this article. Requests to access these datasets should be directed to acoudurierc@gmail.com.

AUTHOR CONTRIBUTIONS

AC-C carried out the study and wrote the paper. SS and ID built a partnership which made the research presented here possible and supervised the project. All authors provided critical feedback and helped shape the research and analysis.

FUNDING

This research was supported by the European Research Council, under the European Union's Seventh Framework Programme (FP7/2007-2013)/ERC Advance Grant agreement no 339442 TransAtlanticILAB and by TGS-NOPEC Geophysical Company (TGS), who has licensed some of their Banda Arc datasets. The IndoDEEP high-resolution multibeam swath bathymetry and 2D seismic reflection data have been acquired as part of the TGS-NOPEC "Indonesia Frontier Basins" (IndoDeep) survey. Seismic reflection data have been visualized using SeisSee program. The morphologic analyses were performed using the ENVI software, and the maps and figures designed using Adobe Illustrator. This work comprises IGP contribution No. 4218.

ACKNOWLEDGMENTS

The authors would like to thank Shamita Das for sharing the seismicity map presented in Figure 7 and Anand Tripathi for initial discussions on the structural architecture and deformation of the Timor region.

SUPPLEMENTARY MATERIAL

The Supplementary Material for this article can be found online at: <https://www.frontiersin.org/articles/10.3389/feart.2021.640928/full#supplementary-material>

REFERENCES

- Audley-Charles, M. (2004). Ocean trench blocked and obliterated by Banda forearc collision with Australian proximal continental slope. *Tectonophysics*, 389, 65–79. doi:10.1016/j.tecto.2004.07.048
- Baillie, P., Fraser, T., Hall, R., and Myers, K. (2004). “Geological Development of Eastern Indonesia and the Northern Australia Collision Zone: A Review,” in *Timor Sea Petroleum Geoscience: Proceedings of the Timor Sea Symposium*, Darwin, Australia, June 19–20, 2003. Editors G. K. Ellis, P. W. Baillie, and T.J. Munson (Jakarta: Northern Territory Geological Survey, Special Publications).
- Baillie, P., and Milne, C. (2014). “New Insights Into Prospectivity and Tectonic Evolution of the Banda Arc: Evidence from Broadband Seismic Data,” in *Proceedings, Indonesian Petroleum Association Thirty-Eighth Annual Convention & Exhibition*, Jakarta, May 2014 (South Jakarta, Indonesia: Indonesian Petroleum Association).
- Barber, P., Carter, P., Fraser, T., Baillie, P., and Myers, K. (2003). “Paleozoic and Mesozoic Petroleum Systems in the Timor and Arafura Seas, Eastern Indonesia”, in *29th Annual Convention Proceedings*, Jakarta, October 14–16, (South Jakarta, Indonesia: Indonesian Petroleum Association), 1–16.
- Becker, J. J., Sandwell, D. T., Smith, W. H. F., Braud, J., Binder, B., Depner, J., et al. (2009). Global Bathymetry and Elevation Data at 30 Arc Seconds Resolution: SRTM30_PLUS. *Mar. Geod.* 32 (4), 355–371. doi:10.1080/01490410903297766
- Bock, Y., Prawirodirdjo, L., Genrich, J. F., Stevens, C. W., McCaffrey, R., Subarya, C., et al. (2003). Crustal Motion in Indonesia from Global Positioning System Measurements. *J. Geophys. Res.* 108 (B8), 2367. doi:10.1029/2001JB000324
- Breen, N. A., Silver, E. A., and Hussong, D. M. (1986). Structural Styles of an Accretionary Wedge South of the Island of Sumba, Indonesia, Revealed by SeaMARC II Side Scan Sonar. *Geol. Soc. Am. Bull.* 97, 1250–1261. doi:10.1130/0016-7606(1986)97<1250:SSOAAW>2.0.CO;2
- Charlton, T. R., Barber, A. J., and Barkham, S. T. (1991). The Structural Evolution of the Timor Collision Complex, Eastern Indonesia. *J. Struct. Geol.* 13, 489–500. doi:10.1016/0191-8141(91)90039-L
- Cummins, P. R. (2017). Geohazards in Indonesia: Earth Science for Disaster Risk Reduction - Introduction. *Geol. Soc. Lond. Spec. Publ.* 441, 1–7. doi:10.1144/SP441.11
- Das, S. (2004). Seismicity Gaps and the Shape of the Seismic Zone in the Banda Sea Region from Relocated Hypocenters. *J. Geophys. Res.* 109, B12303. doi:10.1029/2004JB003192
- Dixon, T. H., Jiang, Y., Malservisi, R., McCaffrey, R., Voss, N., Protti, M., et al. (2014). Earthquake and Tsunami Forecasts: Relation of Slow Slip Events to Subsequent Earthquake Rupture. *Proc. Natl. Acad. Sci. U.S.A.* 111 (48), 17039–17044. doi:10.1073/pnas.1412299111
- Elburg, M. A., Foden, J. D., van Bergen, M. J., and Zulkarnain, I. (2005). Australia and Indonesia in Collision: Geochemical Sources of Magmatism. *J. Volcanol. Geotherm. Res.* 140, 25–47. doi:10.1016/j.jvolgeores.2004.07.014
- Ely, K. S., and Sandiford, M. (2010). Seismic Response to Slab Rupture and Variation in Lithospheric Structure beneath the Savu Sea, Indonesia. *Tectonophysics* 483 (1–2), 112–124. doi:10.1016/j.tecto.2009.08.027
- Fisher, T. L., and Harris, R. A. (2016). Reconstruction of 1852 Banda Arc Megathrust Earthquake and Tsunami. *Nat. Hazards* 83, 667–689. doi:10.1007/s11069-016-2345-6
- Genrich, J. F., Bock, Y., McCaffrey, R., Calais, E., Stevens, C. W., and Subarya, C. (1996). Accretion of the Southern Banda Arc to the Australian Plate Margin Determined by Global Positioning System Measurements. *Tectonics* 15, 288–295. doi:10.1029/95TC03850
- Hall, R. (2009). “Indonesia, Geology,” in *Encyclopedia of Islands*. Editors R. Gillespie and D. Clague (Berkeley, CA: University of California Press), 454–460. doi:10.1525/9780520943728
- Han, S., Bangs, N. L., Carbotte, S. M., Saffer, D. M., and Gibson, J. C. (2017). Links Between Sediment Consolidation and Cascadia Megathrust Slip Behaviour. *Nat. Geosci.* 10, 954–959. doi:10.1038/s41561-017-0007-2
- Harris, R., and Major, J. (2016). “Waves of Destruction in the East Indies: the Wichmann Catalogue of Earthquakes and Tsunami in the Indonesian Region from 1538 to 1877,” in *Geohazards in Indonesia: Earth Science for Disaster Risk Reduction*. Editors P. R. Cummins and I. Meilano (Geological Society, London, Special Publications), 9–46. doi:10.1144/SP441.11
- Harris, R. (2011). “The Nature of the Banda Arc-Continent Collision in the Timor Region,” in *Arc Continent Collision, Frontiers in Earth Sciences*. Editors D. Brown and P. D. Ryan (Berlin, Germany: Springer-Verlag), 163–211.
- Hengesh, J. V., and Whitney, B. B. (2016). Transcurrent Reactivation of Australia’s Western Passive Margin: An Example of Intraplate Deformation from the central Indo-Australian Plate. *Tectonics* 35, 1066–1089. doi:10.1002/2015TC004103
- Hughes, B. D., Baxter, K., Clark, R. A., and Snyder, D. B. (1996). *Detailed processing of seismic reflection data from the frontal part of the Timor trough accretionary wedge, eastern Indonesia*, Geological Society, London: . Special Publications, 106, 75–83. doi:10.1144/GSL.SP.1996.106.01.07
- Karig, D. E., Barber, A. J., Charlton, T. R., Klemperer, S., and Hussong, D. M. (1987). Nature and Distribution of Deformation across the Banda Arc-Australian Collision Zone at Timor. *Geol. Soc. Am. Bull.* 98 (1), 18–32. doi:10.1130/0016-7606(1987)98<18:NADODA>2.0.CO;2
- Keep, M., Clough, M., and Langhi, L. (2002). “Neogene Tectonic and Structural Evolution of the Timor Sea Region, NW Australia,” in *The Sedimentary Basins of Western Australia* 3. Editors M. Keep and S. J. Moss (Perth, Australia: Petroleum Exploration Society of Australia Limited), Vol. 1, 342–353.
- Kodaira, S., Nakamura, Y., Yamamoto, Y., Obana, K., Fujie, G., No, T., et al. (2017). Depth-Varying Structural Characters in the Rupture Zone of the 2011 Tohoku-Oki Earthquake. *Geosphere* 13 (5), 1408–1424. doi:10.1130/GES01489.1
- Kodaira, S., No, T., Nakamura, Y., Fujiwara, T., Kaiho, Y., Miura, S., et al. (2012). Coseismic Fault Rupture at the Trench axis during the 2011 Tohoku-Oki Earthquake. *Nat. Geosci.* 5 (9), 646–650. doi:10.1038/ngeo1547
- Koulali, A., Susilo, S., McClusky, S., Meilano, I., Cummins, P., Tregoning, P., et al. (2016). Crustal Strain Partitioning and the Associated Earthquake Hazard in the Eastern Sunda-Banda Arc. *Geophys. Res. Lett.* 43 (5), 1943–1949. doi:10.1002/2016GL067941
- Li, J., Shillington, D. J., Bécél, A., Nedimović, M. R., Webb, S. C., Saffer, D. M., et al. (2015). Down Dip Variations in Seismic Reflection Character: Implications for Fault Structure and Seismogenic Behavior in the Alaska Subduction Zone. *J. Geophys. Res. Solid Earth* 120 (11), 7883–7904. doi:10.1002/2015JB012338
- Li, J., Shillington, D. J., Saffer, D. M., Bécél, A., Nedimović, M. R., Kuehn, H., et al. (2018). Connections Between Subducted Sediment, Pore-Fluid Pressure, and Earthquake Behavior along the Alaska Megathrust. *Geology* 46 (4), 299–302. doi:10.1130/g39557.1
- Liu, Z. Y.-C., and Harris, R. A. (2013). Discovery of Possible Mega-Thrust Earthquake along the Seram Trough from Records of 1629 Tsunami in Eastern Indonesian Region. *Nat. Hazards* 72 (3), 1311–1328. doi:10.1007/s11069-013-0597-y
- Masson, D. G., Milsom, J., Barber, A. J., Sikumbang, N., and Dwiyanto, B. (1991). Recent Tectonics Around the Island of Timor, Eastern Indonesia. *Mar. Pet. Geol.* 8 (1), 35–49. doi:10.1016/0264-8172(91)90043-Z
- McCaffrey, R., and Nabelek, J. (1984). The Geometry of Back Arc Thrusting along the Eastern Sunda Arc, Indonesia: Constraints from Earthquake and Gravity Data. *J. Geophys. Res.* 89 (NB7), 6171–6179. doi:10.1029/JB089iB07p06171
- Moore, G. F., Bangs, N. L., Taira, A., Kuramoto, S., Pangborn, E., and Tobin, H. J. (2007). Three-Dimensional Splay Fault Geometry and Implications for Tsunami Generation. *Science* 318, 1128–1131. doi:10.1126/science.1147195
- Norvick, M. S. (1979). The Tectonic History of the Banda Arcs, Eastern Indonesia: A Review. *J. Geol. Soc.* 136 (5), 519–526. doi:10.1144/gsjgs.136.5.0519
- Nugroho, H., Harris, R., Lestariya, A. W., and Maruf, B. (2009). Plate Boundary Reorganization in the Active Banda Arc-Continent Collision: Insights from New GPS Measurements. *Tectonophysics* 479 (1–2), 52–65. doi:10.1016/j.tecto.2009.01.026
- Okal, E. A., and Reymond, D. (2003). The Mechanism of Great Banda Sea Earthquake of 1 February 1938: Applying the Method of Preliminary Determination of Focal Mechanism to a Historical Event. *Earth Planet. Sci. Lett.* 216 (1–2), 1–15. doi:10.1016/S0012-821X(03)00475-8
- Olsen, K. M., Bangs, N. L., Tréhu, A. M., Han, S., Arnulf, A., and Contreras-Reyes, E. (2020). Thick, strong Sediment Subduction along South-Central Chile and its Role in Great Earthquakes. *Earth Planet. Sci. Lett.* 538, 116195. doi:10.1016/j.epsl.2020.116195

- Qiu, Q., Hill, E. M., Barbot, S., Hubbard, J., Feng, W., Lindsey, E. O., et al. (2016). The Mechanism of Partial Rupture of a Locked Megathrust: The Role of Fault Morphology. *Geology* 44, 875–878. doi:10.1130/G38178.1
- Rolandone, F., Nocquet, J.-M., Mothes, P. A., Jarrin, P., Vallée, M., Cubas, N., et al. (2018). Areas Prone to Slow Slip Events Impede Earthquake Rupture Propagation and Promote Afterslip. *Sci. Adv.* 4 (1), ea06596. doi:10.1126/sciadv.a06596
- Roosmawati, N., and Harris, R. (2009). Surface Uplift History of the Incipient Banda Arc-Continent Collision: Geology and Synorogenic Foraminifera of Rote and Savu Islands, Indonesia. *Tectonophysics* 479 (1–2), 95–110. doi:10.1016/j.tecto.2009.04.009
- Ruff, L. J. (1989). Do trench Sediments Affect Great Earthquake Occurrence in Subduction Zones?. *Pure Appl. Geophys.* 129, 263–282. doi:10.1007/978-3-0348-9140-0_9
- Sandiford, M. (2008). Seismic Moment Release during Slab Rupture beneath the Banda Sea. *Geophys. J. Int.* 174 (2), 659–671. doi:10.1111/j.1365-246X.2008.03838.x
- Scholz, C. H., and Campos, J. (2012). The Seismic Coupling of Subduction Zones Revisited. *J. Geophys. Res.* 117, B05310. doi:10.1029/2011JB009003
- Scotney, P. M., Roberts, S., Herrington, R. J., Boyce, A. J., and Burgess, R. (2005). The Development of Volcanic Hosted Massive Sulfide and Barite–Gold Orebodies on Wetar Island, Indonesia. *Miner. Deposita* 40, 76–99. doi:10.1007/s00126-005-0468-x
- Shulgin, A., Kopp, H., Mueller, C., Lueschen, E., Planert, L., Engels, M., et al. (2009). Sunda-Banda Arc Transition: Incipient Continent-Island Arc Collision (Northwest Australia). *Geophys. Res. Lett.* 36, L10304. doi:10.1029/2009GL037533
- Singh, S. C., Hananto, N., Mukti, M., Permana, H., Djajadihardja, Y., and Harjono, H. (2011). Seismic Images of the Megathrust Rupture during the 25th October 2010 Pagai Earthquake, SW Sumatra: Frontal Rupture and Large Tsunami. *Geophys. Res. Lett.* 38 (16), L16313. doi:10.1029/2011GL048935
- Tréhu, A. M., Hass, B., de Moor, A., Maksymowicz, A., Contreras-Reyes, E., Vera, E., et al. (2019). Geologic Controls on Up-Dip and Along-Strike Propagation of Slip during Subduction Zone Earthquakes from a High-Resolution Seismic Reflection Survey across the Northern Limit of Slip during the 2010 Mw 8.8 Maule Earthquake, Offshore Chile. *Geosphere* 15 (6), 1751–1773. doi:10.1130/GES02099.1
- Van Bergen, M. J., Erfan, R. D., Sriwana, T., Suharyono, K., Poorter, R. P. E., Varekamp, J. C., et al. (1989). Spatial Geochemical Variations of Arc Volcanism Around the Banda Sea. *Neth. J. Sea Res.* 24 (2–3), 313–322. doi:10.1016/0077-7579(89)90157-9
- Varekamp, J. C., Van Bergen, M. J., Vroon, P. Z., Poorter, R. P. E., Wirakusumah, A. D., Erfan, R., et al. (1989). Volcanism and Tectonics in the Eastern Sunda Arc, Indonesia. *Neth. J. Sea Res.* 24 (2–3), 303–312. doi:10.1016/0077-7579(89)90156-7
- von Huene, R., Miller, J. J., and Krabbenhoft, A. (2019). The Shumagin Seismic gap Structure and Associated Tsunami Hazards, Alaska Convergent Margin. *Geosphere* 15 (2), 324–341. doi:10.1130/GES01657.1
- Watson, S. J., Mountjoy, J. J., Barnes, P. M., Crutchley, G. J., Lamarche, G., Higgs, B., et al. (2020). Focused Fluid Seepage Related to Variations in Accretionary Wedge Structure, Hikurangi Margin, New Zealand. *Geology* 48, 56–61. doi:10.1130/G46666.1
- Watt, C. J. (1976). *Geophysical Results of the Timor Trough: Australia Bur.* Mineral Resources, Geology and Geophysics, 15.
- Wichmann, A. (1918). “Die Erdbeben des indischen Archipels bis zum Jahre 1857,” in *Verhandelingen der Koninklijke akademie van wetenschappen te Amsterdam*. Editor Müller, J. (Amsterdam: Johannes Müller), Vol. 4, 193.

Conflict of Interest: Author ID was employed by the company TGS GPSI.

The remaining authors declare that the research was conducted in the absence of any commercial or financial relationships that could be construed as a potential conflict of interest.

Copyright © 2021 Coudurier-Curveur, Singh and Deighton. This is an open-access article distributed under the terms of the Creative Commons Attribution License (CC BY). The use, distribution or reproduction in other forums is permitted, provided the original author(s) and the copyright owner(s) are credited and that the original publication in this journal is cited, in accordance with accepted academic practice. No use, distribution or reproduction is permitted which does not comply with these terms.